



Published in final edited form as:

Brain Struct Funct. 2019 June ; 224(5): 1831–1843. doi:10.1007/s00429-019-01875-z.

Controllable stress elicits circuit-specific patterns of prefrontal plasticity in males, but not females

Michael V. Baratta¹, Tina M. Gruene², Samuel D. Dolzani¹, Lauren E. Chun¹, Steven F. Maier¹, and Rebecca M. Shansky²

¹Department of Psychology and Neuroscience, University of Colorado Boulder, 2860 Wilderness Place, Boulder, CO 80301

²Department of Psychology, Northeastern University, 360 Huntington Ave, 125 NI, Boston, MA 02115

Abstract

Actual or perceived behavioral control during a traumatic event can promote resilience against future adversity, but the long-term cellular and circuit mechanisms by which this protection is conferred have not been identified. Clinical outcomes following trauma exposure differ in men and women, and therefore it is especially important in preclinical research to dissect these processes in both males and females. In male adult rats, an experience with behavioral control over tail shock (“escapable stress”, ES) has been shown to block the neurochemical and behavioral outcomes produced by later uncontrollable tail shock (“inescapable stress”, IS), a phenomenon termed “behavioral immunization.” Here we determined whether behavioral immunization is present in females. Unlike males, the stress buffering effects of behavioral control were absent in female rats. We next examined the effects of ES and IS on spine morphology of dorsal raphe nucleus (DRN)-projecting prelimbic (PL) neurons, a circuit critical to the immunizing effects of ES in males. In males, IS elicited broad, non-specific alterations in PL spine size, while ES elicited PL-DRN circuit-specific spine changes. In contrast, females exhibited broad, non-specific spine enlargement after ES but only minor alterations after IS. These data provide evidence for a circuit-specific mechanism of structural plasticity that could underlie sexual divergence in the protective effects of behavioral control.

Corresponding Author: Rebecca M. Shansky, Department of Psychology, Northeastern University, 360 Huntington Ave, 125 NI, Boston, MA 02115, r.shansky@northeastern.edu, phone: (617) 373-6819.

Publisher's Disclaimer: This Author Accepted Manuscript is a PDF file of an unedited peer-reviewed manuscript that has been accepted for publication but has not been copyedited or corrected. The official version of record that is published in the journal is kept up to date and so may therefore differ from this version.

Conflict of Interest

The authors declare no conflict of interest.

Ethical approval

All applicable international, national, and/or institutional guidelines for the care and use of animals were followed. All procedures performed in studies involving animals were in accordance with the ethical standards of the institution or practice at which the studies were conducted.

Keywords

Coping; medial prefrontal cortex; dorsal raphe nucleus; dendritic spines; structural plasticity; learned helplessness

Introduction

Most people will experience a traumatic event in their lifetime, but long-term mental health outcomes in trauma-exposed populations vary (Yehuda and LeDoux, 2007). Thus, determining the situational and neurobiological factors that confer risk or resilience is a critical objective for preclinical research. One notable predictor of resilience is the presence of either perceived or actual behavioral control over a stressor (Charney, 2004; Shapiro et al., 1996; Southwick and Charney, 2012), yet how an initial experience with behavioral control leads to long-lasting protection on a mechanistic level is not fully understood.

In rodents, the impact of stressor controllability on the brain and behavior has typically been studied using an escapable stress (ES)/yoked inescapable stress (IS) model (Maier, 2015). Decades of research using this paradigm have demonstrated that in male rats, IS exposure results in numerous behavioral outcomes, including decreased juvenile social exploration (JSE; Christianson et al., 2008), exaggerated fear conditioning (Baratta et al., 2007; Maier et al., 1995), and impaired shuttlebox escape (Amat et al., 2001; Maier and Seligman, 1976) that do not occur in physically identical ES (Maier and Watkins, 2005). These behavioral changes, which are often termed “learned helplessness” effects, have been linked to IS-induced activation of the serotonergic (5-HT) dorsal raphe nucleus (DRN). IS produces greater 5-HT release in the DRN and its projection regions than does equal ES, and this activation is a critical mediator of the behavioral effects of IS through downstream 5HT signaling in brain regions like the striatum and amygdala (Christianson et al., 2010; Strong et al., 2011). Furthermore, in a related paradigm termed “behavioral immunization”, an initial experience with ES buffers males against DRN 5-HT activation and behavioral outcomes of *future* IS exposure (Amat et al., 2006a), as well as other uncontrollable stressors, such as social defeat (Amat et al., 2010). Thus, experience with ES has a long-lasting “immunizing” effect against future stressors.

In males, ES-induced behavioral immunization requires activation of prelimbic (PL) projections to the DRN both at the time of initial ES *and* during subsequent IS (Amat et al., 2006b; Baratta et al., 2009). These data suggest that ES elicits a selective strengthening of the PL-DRN circuit that leads to subsequent recruitment during future IS, potentially through rapid changes in dendritic spine morphology. However, despite robust evidence that other stressors can cause dendritic remodeling in the PL (Garrett and Wellman, 2009; Radley et al., 2008, 2013; Shansky and Morrison, 2009), the impact of controllability on structural plasticity has not been investigated.

Another gap in our understanding of stressor controllability has been whether the protective effects of ES are present in females. Prior female “learned helplessness” studies either did not include a group for which the stressor is controllable (Heinsbroek et al., 1991; Kirk and Blampied, 1985; Steenbergen et al., 1990) or did not observe IS effects in females relative to

non-stressed home cage (HC) control subjects (Dalla et al., 2008). In either case, the impact of behavioral control on stressor outcome cannot be determined, which is the focus here. We recently reported that although female subjects receiving ES readily learn the controlling escape response, they still later exhibit the same decreased JSE and potentiated freezing as do IS females (Baratta et al., 2018). Furthermore, behavioral control failed to activate the PL-DRN projection, as it does in males. However, this study did not investigate ES immunization against future IS exposure.

The stress-buffering effects of ES in males rely on selective activation of PL-DRN circuitry, and so we would therefore expect to observe a) a failure of ES in females to produce behavioral immunization against subsequent IS, and b) circuit-specific plasticity after ES in males, but not females. Here we provide support for both of these hypotheses, identifying a potential cellular mechanism by which stressor controllability can confer lasting changes in key prefrontal circuits.

Materials and methods

Subjects

Adult male (~300g) and female (~250g) Sprague–Dawley rats (Envigo, Indianapolis, IN, USA) were pair housed on a 12-h light–dark cycle (lights on at 0600 h). Food (standard laboratory chow) and water were available *ad libitum*. Rats were allowed to acclimate to colony conditions for at least one week prior to experimentation. Stress treatment and behavioral testing were conducted between 0900 and 1400 h. Experimental groups for Study 1 (behavioral immunization) are designated by first stress treatment/second stress treatment, which occurred 7 days later: HC/HC (male n=10, female n=8); HC/IS (male n=10, female n=9); IS/IS (male n=10, female n=8); ES/IS (male n=11, female n=7). Experimental groups for Study 2 (structural plasticity) were as follows: HC (male: n=9, female n=7); ES (male n=9, female n=6); IS (male n=8, female n=9). All experiments were approved by the Institutional Animal Care and Use Committee of the University of Colorado Boulder in compliance with the National Institutes of Health *Guide for the Care and Use of Laboratory Animals*.

Study 1: Behavioral immunization

Wheel-turn ES/yoked IS procedure: For manipulation of stressor controllability, subjects were run in a same sex triad design, as described previously (Amat et al., 2010; Baratta et al., 2007; Christianson et al., 2009). One subject of each triad received ES (turning the wheel at the front of the chamber terminated each tailshock), a second received yoked IS, and a third received no tailshock and remained in its home cage (HC). Each ES and IS rat was placed in a Plexiglas box (14 × 11 × 17 cm) with a wheel mounted in the front. The tail was secured to a Plexiglas rod extending from the back of the box, and affixed with two copper electrodes and electrode paste. The wheel-turn ES/yoked IS procedure consisted of a single session of 100 trials of tailshock (33 × 1.0, 33 × 1.3, 34 × 1.6 mA) on a variable interval 60-s schedule. Initially, the shock was terminated by a quarter turn of the wheel. When trials were completed in less than 5 s, the response requirement was increased by one-quarter turn of the wheel, up to a maximum of four full turns of the wheel. The requirement

was reduced if the trial was not completed in less than 5 s. If the trial was not completed in 30 s, the shock was terminated and the requirement was reduced to one-quarter turn of the wheel. For yoked IS rats, the onset and offset of each tailshock is identical to that of the ES partner. Sessions lasted 110 minutes

Behavioral immunization: One week after the wheel-turn ES/yoked IS procedure (ES, IS, or HC), subjects received a single session of 100 trials of uncontrollable tailshocks (5 s duration each) in restraint tubes at an average inter-trial interval of 60 s. Current intensity varied between 1.0 and 1.6 mA as described above.

Juvenile social exploration (JSE): Twenty-four hours before the first stress treatment rats were removed from the colony and transferred to a testing room where a baseline interaction measure was taken. Each experimental adult rat was allocated to a separate plastic cage with a wire lid and bedding in a brightly lit testing room. After 60 min the adult rat was added to an interaction cage that contained a juvenile stimulus rat (28–35 days old Sprague-Dawley, matched to sex of adult rat). Investigative behaviors, including sniffing, pinning, and allogrooming, initiated by the adult rat were timed by an observer blind to experimental condition. Following the 3-min JSE test, which occurred 24 h following the second stress treatment (behavioral immunization) the adult rat was returned to its home cage. Juveniles were used for multiple tests, but never more than once for the same adult rat. Total interaction time was calculated.

Shock-elicited freezing: Shock-elicited freezing was assessed in two-way shuttle boxes (50.8 × 25.4 × 30.48 cm; Coulbourn Instruments, Holliston, MA, USA) as previously described (Amat et al., 2005; Strong et al., 2011). The day after the second stress treatment (behavioral immunization) and two hours following the JSE test, subjects were placed into shuttle boxes and allowed to explore for 5 min. Rats then received two 0.7 mA foot shocks delivered through both sides of the grid floor. Foot shocks were terminated when the subject crossed over to the opposite side of the shuttle box through a small archway (fixed ratio 1, FR-1). Following the second FR-1 trial, shock-elicited freezing was observed for 20 min. Shock-elicited freezing is a measure of fear conditioned to cues present in the shuttle box. Each subject's behavior was scored every 10 s as being either freezing or not freezing. Freezing was defined as the absence of all movement except that required for respiration.

Study 2: Structural plasticity in the PL-DRN circuit

Retrograde tracer surgery: Stereotaxic surgeries for retrobead delivery into the DRN were carried out under Isoflurane (5% induction, 2% maintenance in 2.5 L/min O₂; Piramal Critical Care, Bethlehem, PA, USA) anesthesia, as previously described (Baratta et al., 2018, 2009). A stainless steel needle with beveled tip (31 gauge; Hamilton Company, Reno, NV, USA) was directed to the DRN (A/P: -8.0 and D/V: -6.7 mm from skull) and green fluorescent retrobeads (Lumafluor, Durham, NC, USA) (in 0.9% sterile saline) was infused at a rate of 0.1 µl/min (0.3 µl total volume) using a UMP3 microinjection pump (World Precision Instruments, Sarasota, FL, USA). The retrograde tracer was allowed to diffuse for an additional 10 min before the needle was withdrawn and the incision was sealed with VetBond (3M, St. Paul, MN, USA). Following surgery, subjects received subcutaneous

injections of a nonsteroidal anti-inflammatory for analgesia (meloxicam, 0.5 mg/kg; Vetmedica, St. Joseph, MO, USA) and an antibiotic (CombiPen-48, 0.25 ml/kg; Bimeda, Oakbrook Terrace, IL, USA). Subjects remained in a recovery box with heating pad until ambulatory before returning to the colony. Subjects were given 10 to 14 days to recover from surgery before the wheel-turn ES/yoked IS procedure.

Euthanasia and tissue preparation: Twenty-four hours following the last tail shock of the wheel-turn ES/yoked IS procedure, subjects (ES, IS, HC) were deeply anesthetized with an overdose of anesthesia and transcardially perfused first with ice-cold 1% paraformaldehyde followed by 4% paraformaldehyde in 0.1 M phosphate buffer (PB). Brains were extracted and post-fixed in 4% paraformaldehyde in PB for 4 hr, then placed in 0.1% sodium azide in 0.1 M phosphate buffered saline at 4 °C until 250 μ m sections were collected on a vibrating microtome.

Iontophoretic microinjections: All tissue processing, imaging, and spine analyses were carried out by an experimenter blind to the sex and stress condition of each subject. Fixed brains were sectioned at 250 μ m on a vibrating microtome (Leica Microsystems, Inc, Buffalo Grove, Illinois), and PL-containing sections selected for microinjections. Retrogradely-labeled PL neurons and unlabeled neighboring neurons were visualized on a Zeiss Axio Examiner A.1 microscope (Zeiss Microscopy, Thornwood, New York). Iontophoretic microinjections of fluorescent dye Lucifer Yellow were targeted to PL layer V pyramidal neurons using a DC current of 5–10 nA for 10–15 minutes, followed by 2 minutes at 15 nA until distal processes were filled and no further loading was observed (Gruene et al., 2016, 2015; Shansky et al., 2009). Sections were mounted on microscope slides with added seal spacers to prevent morphological distortions due to the weight of the cover glass. Then, sections were coverslipped using Vectashield (Vector Laboratories) mounting medium.

Imaging and dendritic spine segment analysis: Five to seven PL-DRN projecting neurons and five to seven unlabeled neurons per animal were included in the analysis. From each neuron 2 proximal (less than 100 μ m from the cell body) and 2 distal (more than 100 μ m from the cell body) segments were sampled from basal dendrites, for a total of 4 segments per neuron. Dendritic segments were chosen based on the following criteria: 1) they were within 80 μ m from the cover glass due to the working range of the microscope lens, 2) they showed no overlap with other dendritic segments, 3) they were mostly parallel to the surface of the tissue. All images were acquired using an Olympus FV1000 confocal microscope (Optical Analysis Corporation, Nashua, New Hampshire). Once selected, segments were imaged using a 100x oil lens, 1.4 NA, zoom of 3.7 and 0.33 μ m step size. Using a 1024 \times 1024 raster these settings resulted in a resolution of 0.033 μ m \times 0.033 μ m \times 0.33 μ m per pixel. Z-stacks were acquired at 2 μ s/pixel, with a Kalmann filter of 4, using a 458 argon laser at 30% power, and between 620–750 HV. Raw Z-stacks were deconvolved with AutoQuant (Media Cybernetics, Rockville, Maryland) and analyzed for spine number (density), shape (thin or mushroom), head diameter, and distance to neighboring spines (clustering) using NeuronStudio software (Computational Neurobiology and Imaging Center, New York, New York). NeuronStudio is an automated tool for unbiased assessment of spine morphology metrics. It determines spine type by calculating the ratio of each

spine's head width to neck width. Spines whose head/neck width ratios are greater than 1.5 are classified as mushroom spines, and those below are thin (Adrian et al., 2017).

Data processing and statistical analysis

The primary goal of these studies was to evaluate whether behavioral control modulates stress-induced changes in behavior and plasticity. The multiple stress groups and circuit conditions made it impractical to power these studies so that 3-way ANOVAs could be conducted. Our goal was not to determine whether IS or ES had different effects in males and females, but rather whether IS and ES led to different outcomes within males and within females. Therefore, all data were analyzed separately for each sex, and are reported as such except where noted. Behavioral data were analyzed with 1- and 2-way ANOVAs where appropriate, followed by corrected Bonferroni post-hoc tests when main effects or interactions were observed. Spine densities for labeled and unlabeled neurons were first averaged by neuron and then by animal, and then a mixed-design ANOVA was performed to test for effects of circuit and stress.

Although spine density (spines/ μm of dendritic length) is arguably the most common measure of experience-dependent plasticity (Farrell et al., 2015; McEwen and Morrison, 2013; Shansky and Morrison, 2009), more subtle alterations in dendritic structure, like changes in spine size and clustering can also reflect shifts in synaptic strength and functioning (Chen et al., 2016; Frank et al., 2018; Kasai et al., 2003). We therefore took advantage of the large spine samples we collected to estimate spine populations, and compared distributions of head diameters and clustering between groups. D'Agostino & Pearson omnibus normality test showed that head diameter sizes are not normally distributed ($p < 0.0001$ for each group), confirming that population distributions, rather than group means, are more meaningful and informative.

Spine head diameter and clustering analyses and plotting were performed using Python 3.5 and its relevant packages (numpy, pandas, scikit learn, scipy, matplotlib, seaborn). Neuronstudio output files (.txt) were combined for each experimental group and head diameters for thin and mushroom spines and distance to nearest other spine were extracted. To assess thin spine clustering, Euclidian distances were first calculated for each spine per dendritic segment (Pereira et al., 2014). Then, distances of each spine to its closest neighbor were normalized to "expected" average distance based on the spine density of each segment. Lastly, normalized minimum distances were combined for PL-DRN and unlabeled neurons of each experimental group. Kolmogorov-Smirnov (KS) tests were used to statistically evaluate group differences in cumulative distributions for both measures.

For improved visualization of group comparisons, we generated Kernel density estimates (Kde) of spine populations for each experimental group (Fig. 3E), which we then converted to "difference plots" based on Kde data (Fig. 3F), plotting each stress group against normalized home cage controls. We believe that this allows a more easily appreciable characterization of population-level shifts in size and clustering than traditional graphic representations (e.g. cumulative distribution or Kde plots), which poorly convey the magnitude of group differences. The code for generating these plots is freely available at

<https://github.com/TinaGruene/spine-analysis>. Cumulative distribution and Kde plots can be found in Supplementary Figures 1–4.

Results

Study 1. Escapable stress (ES) does not protect female rats from the effects of later inescapable stress (IS)

We first tested for the ability of ES to protect against the behavioral effects of subsequent IS given 1 week later. This phenomenon, called “behavioral immunization” has been previously demonstrated in males and relies on activation of PL projections to the DRN, which inhibit IS-induced DRN 5-HT activation through synapses on GABAergic interneurons (Amat et al., 2006a; Jankowski and Sesack, 2004; Varga et al., 2001). Male and female rats were exposed to ES, IS, or HC and then one week later received IS in a restraint tube. Half of the HC subjects were not given subsequent IS (HC/HC) to provide a no stress comparison group. ES male and female subjects quickly reached the maximum number of wheel turns required to terminate the shock during ES (Fig. 2A, t-test $p=0.91$) and maintained optimal escape responses throughout the 100-trial session (Fig. 2B, non-significant trend to effect of sex: $F_{1,17}=4.3$, $p=0.053$), suggesting that there were no overall sex differences in the acquisition nor motivation to escape across trials. We found similar results in our Study 2 cohort (Fig. 2C, t-test $p=0.99$; Fig. 2D, $F_{1,13}=0.02$, $p=0.87$).

Twenty-four hours after the final IS session, animals received a JSE test. Compared to HC/HC males, HC/IS and IS/IS animals spent less time interacting with the juvenile animal (Fig. 2E, 1-way ANOVA $F_{3,37}=5.6$, $p=0.003$; Corrected Bonferroni: HC/HC vs. HC/IS $p=0.004$; HC/HC vs. IS/IS $p=0.004$). ES/IS animals spent an intermediate amount of time interacting (Corrected Bonferroni vs. HC/HC $p=0.25$; vs. HC/IS $p=0.25$; vs. IS/IS $p=0.24$), suggesting that ES can at least partially prevent or blunt the effects of subsequent IS in males.

Two hours after JSE, animals were placed in a two-way shuttlebox and exposed to two escapable FR-1 foot shocks. Prior stress exposure did not affect mean latency to escape, and all animals escaped well under the 30s limit (Fig. 2F; 1-way ANOVA $F_{3,31}=2.3$, $p=0.095$). That is, all groups received the same duration of footshocks. After the 2nd footshock, animals remained in the shuttlebox for 20 minutes and post-shock freezing was observed. As is typical, IS potentiated freezing (Fig. 2G), and importantly, this potentiation was completely blocked by prior ES exposure. We found a significant stress x trial interaction (2-way ANOVA: $F_{27,297}=2.7$, $p<0.0001$), and corrected Bonferroni post-hoc tests revealed that ES/IS animals reduced freezing significantly faster than IS/IS (block 6, $p=0.01$; block 7, $p<0.0001$) and HC/IS animals (block 7, $p=0.006$; block 8, $p=0.01$). As previously shown, these data indicate that in male rats ES blunts the behavioral consequences of future IS.

In females, however, no protective immunizing effects of ES were observed. All stress-exposed animals exhibited a reduction in time spent interacting in the JSE test compared to HC/HC, regardless of controllability condition (Fig. 2H; 1-way ANOVA $F_{3,27}=7.3$, $p=0.001$; corrected Bonferroni's HC/HC vs. HC/IS $p=0.004$; vs. IS/IS $p=0.003$; vs. ES/IS $p=0.001$). Similar to males, there was no significant group effect in shuttlebox FR-1 escape latency

(Fig. 2I; 1-way ANOVA $F_{3,27}=2.7$, $p=0.07$). However, we did find a main effect of stress in post-shock freezing (Fig. 2J; 2-way ANOVA $F_{3,31}=3.1$, $p=0.04$), which corrected Bonferroni's tests suggest were due to accelerated reduction in freezing in HC/HC animals ($p=0.04$ vs. IS/IS block 6–8; $p=0.01$ block 9–10).

Together, these data show that despite comparable wheel-turn escape responding during ES in males and females, ES has long-term protective effects in males that we do not observe in females. To identify a potential cellular mechanism underlying this difference, we next examined ES- or IS-induced structural plasticity in the PL-DRN circuit.

Study 2. Escapable and inescapable stress induce discrete patterns of PL plasticity in males and females.

The experimental approach we used here is illustrated in Figure 3: First, we injected fluorescent retrobeads into the DRN (Fig. 3A). After 10 days subjects received ES, yoked IS, or HC control treatment, euthanized 24 hr later, and retrobead-positive layer V PL neurons and unlabeled neighbors were iontophoretically filled with Lucifer Yellow (Fig. 3B). This time point was chosen in order to observe the initial PL-DRN circuit response to ES or IS and to be comparable to other studies of acute stress effects on dendritic spines (Nava et al., 2015). Future studies will investigate potential slow-developing alterations in dendritic structure after ES or IS.

Dendritic segments from the basal arbor were selected (Fig. 3C) for confocal imaging (Fig. 3D). We then calculated population distributions for spine head diameter (Fig. 3E), comparing ES and IS against HC for both mushroom and thin spines. From these comparisons, we generated a difference plot (Fig. 3F) to better visualize how spine populations in ES or IS animals differed from those in HC animals. Fig. 3E–G illustrates this process using PL-DRN mushroom spines in ES males, which exhibited an increase in large-sized mushroom spines (Fig. 3G, left: HC, right: ES).

We first examined the effects of ES and IS on spine density in labeled and unlabeled neurons (Figure 4). Mixed-design ANOVA with stress condition as between animal factor and PL-DRN and unlabeled neurons as within animal factor revealed a main effect of circuit in mushroom spine densities without interaction in males (Figure 4A; stress: $F(2,23)=2.133$, $p=0.1413$; circuit: $F(1,23)=5.737$, $p=0.0251$, interaction: $F(2,23)=0.98328$, $p=0.4078$), but no significant effects on thin spine densities (Figure 4C, stress: $F(2,23)=1.016$, $p=0.3777$; circuit: $F(1,23) = 0.8866$, $p=0.3564$; interaction: $F(2,23)=0.7828$, $p=0.4689$). In females, there was no effect of circuit on mushroom spine densities (Figure 4B; stress: $F(2,19)=0.4753$, $p=0.6289$; circuit: $F(1,19)=3.735$, $p=0.0683$; interaction: $F(2,19)=0.5645$, $p=0.5779$), but a main effect of circuit in thin spine densities without interaction (Figure 4D; stress: $F(2,19)=0.08943$, $p=0.9148$; circuit: $F(1,19)=10.73$, $p=0.004$; interaction: $F(2,19)=0.04566$, $p=0.9555$). These effects are small, and without stress interactions this result is likely not meaningful for the research questions at hand.

We next examined the effects of stress on spine size. In males, IS induced a robust increase in both mushroom and thin spine head diameter that was not circuit-specific (Fig. 5A, left. IS vs. HC: PL-DRN mushroom KS $D = 0.052$, $p<0.02$; PL-DRN thin KS $D = 0.045$,

$p < 0.0001$; unlabeled mushroom KS D = 0.035, $p = 0.06$; unlabeled thin KS D = 0.032, $p < 0.0001$). In contrast, IS-induced spine changes in females were only observed in unlabeled mushroom spines (Fig. 5A, right. IS vs. HC: KS D = 0.066, $p = 0.0002$). Mushroom spines on DRN-projecting PL neurons trended towards an IS-induced increase in size but did not reach significance (KS D = 0.043, $p = 0.08$).

ES induced a very different pattern of spine changes. In males, we observed a circuit-specific head diameter increase exclusively in PL-DRN mushroom spines (Fig. 5B, left. ES vs. HC: KS D = 0.047, $p = 0.04$). In females, however, ES induced significant increases in spine size in both thin and mushroom spines, regardless of circuit (Fig. 5B, right. ES vs. HC: PL-DRN mushroom; KS D = 0.087, $p < 0.0001$; PL-DRN thin: KS D = 0.036 $p = 0.003$; unlabeled mushroom KS D = 0.047, $p = 0.04$; unlabeled thin: KS D = 0.034, $p = 0.0005$).

Finally, we investigated thin spine clustering, which followed similar patterns to that of spine head diameter. Specifically, we observed increased clustering in PL-DRN, but not unlabeled, neurons in ES males compared to HC males (Fig 6A, left; KS D = 0.032, $p < 0.001$). In addition, we again observed global alterations in IS males in both PL-DRN and unlabeled neurons (Fig 6B, left; PL-DRN: KS D = 0.022, $p < 0.05$; unlabeled: KS D = 0.037, $p < 0.0001$). In females, ES increased clustering in both PL-DRN and unlabeled neurons (Fig 6A, right; PL-DRN: KS D = 0.032, $p < 0.005$; Fig 6B, right; unlabeled: KS D = 0.033, $p < 0.0003$). Interestingly, IS females exhibited a significant *decrease* in clustering in both PL-DRN and unlabeled neurons (PL-DRN: KS D = 0.032, $p = 0.001$; unlabeled: KS D = 0.022, $p < 0.02$).

Discussion

The work described here represents the first investigation into the potential for controllable vs. uncontrollable stress to elicit discrete patterns of structural plasticity, which may contribute to long-term adaptive or maladaptive behavioral outcomes. We found that while IS resulted in decreased JSE and potentiated post-shock freezing in males and females, ES protected only males from the effects of subsequent IS, suggesting that ES confers neither short term (Baratta et al, 2018) nor immunizing effects in females. Furthermore, ES elicited PL-DRN circuit-specific changes in spine head diameter and clustering in males, but global, non-specific changes in females. These neuroanatomical measures are associated with synaptic strengthening and improved cognition (Frank et al., 2018; Fu et al., 2012; Pereira et al., 2014), and therefore our findings provide evidence for a potential cellular mechanism by which controllable stress confers long-term protection in males, but not females. As we discuss below, the structural alterations we observed may reflect a selective increase in PL-DRN excitability in ES males, thereby facilitating DRN silencing during future IS exposure and immunizing against the behavioral consequences of IS.

Our behavioral findings here build on our recent report that behavioral control does not protect females from the short term effects of shock exposure in measures of JSE and shock-induced freezing (Baratta et al., 2018). Prior work in males has shown that behavioral control (ES) blocks the behavioral effects of the shock stressor by activating DRN-projecting PL neurons that inhibit DRN 5-HT activation during shock exposure (Amat et al., 2005). In

females, however, behavioral control does not activate DRN-projecting PL neurons, and so, stress induced DRN 5-HT activation is not blunted (Baratta et al., 2018). Thus, despite the existence of PL-DRN circuitry in females and the ability of female rats to acquire the controlling wheel-turn response, the ES experience engages the PL differently in males and females. Here we add to these findings, extending the impact of ES failure in females to behavioral immunization, which we only observed in males.

The behavioral immunization phenomenon suggests that the initial ES experience may induce synaptic changes that ultimately shape an animal's response to subsequent challenges. As discussed above, PL activity both at the time of 1) the original ES experience and 2) subsequent IS is necessary for the immunizing effects of ES. That is, prior experience with behavioral control alters the PL-DRN pathway in such a way that later uncontrollable stressors, which normally don't activate the PL-DRN, now do so, thereby inhibiting 5-HT release in the DRN and its projection regions, preventing the behavioral sequelae typically observed following IS (e.g. exaggerated freezing, reduced juvenile social exploration).

We therefore first sought to investigate structural changes around the initial experience with ES. Prior work has found that ES and IS differentially activate DRN-projecting PL neurons, but equally activate unlabeled PL neurons (Baratta et al., 2009). Consistent with this pattern, here we found that ES in males induced enlarged mushroom spines and thin spine clustering only in the DRN-projecting PL neurons, but not in unlabeled PL neurons. In contrast to ES, IS in males induced a broad increase in mushroom and thin spine size in both labeled and unlabeled neurons, also consistent with our previous report.

We do not yet know the mechanisms that drive these structural effects. One possibility is that the increased head diameters of thin and mushroom spines in IS males are a consequence of stress-induced, general enhancement of glutamate activity. Acute foot shock stress increases glutamate release in PFC via glucocorticoid signaling (Musazzi et al., 2010; Popoli et al., 2011), and glutamatergic stimulation of spines has been shown to increase spine volume and enhance AMPA currents (Matsuzaki et al., 2004; Tanaka et al., 2008). This global potentiation of synapses may not directly lead to the behavioral effects of IS we observe here, but could be a consequence of stress that indirectly affects other processes. Supporting this possibility are findings that a local infusion of muscimol, the protein synthesis inhibitor anisomycin, or a MEK inhibitor into the PL before ES or IS prevents the behavioral immunization effects of ES, but not IS-related behavioral deficits (Amat et al., 2005, 2006a; Christianson et al., 2014). Therefore, preferential recruitment of PL-DRN neurons by ES may also reflect suppressed activity at other PL neural populations. In this way, the observed changes in mushroom spine size and thin spine clustering could be both a result of enhanced circuit activity, and contribute to the long-term effects of ES. Because increased head diameter can reflect insertion of AMPA receptors into the cellular membrane (Matsuzaki et al., 2001), ES may selectively strengthen PL-DRN synapses in males in order to enable behavioral immunization during subsequent IS exposure.

In females, the lack of circuit-specific plasticity after ES is in line with our current behavioral findings that ES does protect against subsequent IS, as well as our previous report that ES does not selectively engage DRN-projecting PL neurons as it does in males (Baratta

et al., 2018). Interestingly, the non-specific increases in both mushroom and thin spine head size and thin spine clustering we observed in ES females are most similar to the effects we observed in males after IS, perhaps shedding light on why ES fails to confer future behavioral protection to females.

Despite ES failing to engage the PL-DRN projection in females, recent work suggests that this circuit is still capable of functioning in a manner similar to that in males. First, pharmacological activation of the PL with picrotoxin before either IS or ES prevents JSE deficits in females (Baratta et al., 2018). Second, ketamine treatment in females selectively increases activity in the PL-DRN pathway and prevents IS-related JSE deficits, an effect that can be reversed with chemogenetic inhibition of the PL-DRN pathway (Dolzani et al., 2018). Therefore, PL-DRN neurons in the female brain appear to have protective potential in behavioral tests known to be sensitive to ES in males, but under our current ES/IS parameters, behavioral control is insufficient in females to overcome the detrimental effects of stress exposure. Future work will determine whether a less protracted ES experience (e.g., a reduced shock regimen) could lead to more “male-like” behavioral and physiological outcomes in females.

In conclusion, we report here that both controllable and uncontrollable stress induce discrete, circuit-specific patterns of structural plasticity in males and females that may be related to differential behavioral outcomes. Whether these neuroanatomical and behavioral observations are causally linked remains to be interrogated experimentally, but new genetic tools like photoactivatable Rac1 (Hayashi-Takagi et al., 2015) make such an investigation technically feasible, and we look forward to addressing this question in future studies. One limitation of the current work is that we do not know the projection targets of the PL neurons included in our “unlabeled” populations, and we cannot rule out the possibility that these include DRN-projecting PL neurons that did not take up the retrograde tracer. Additionally, the potential contribution of downstream PL-DRN collaterals to our effects is unknown. Further dissection of circuit-specific effects of stress on prefrontal plasticity will be an important future step in determining the mechanisms by which stress affects a wide variety of behaviors, including cognition, emotion regulation, and substance abuse (McEwen and Stellar, 1993). Lastly, our current data add to a growing body of evidence showing that stress affects the male and female brain differently (Bangasser and Wicks, 2017; Farrell et al., 2015), an area of research with clear clinical implications. Because stress related mental illnesses differ in both prevalence and symptomatology in men and women (Breslau and Kessler, 2001), a better understanding of the situational and neurobiological factors that determine long-term outcomes in both sexes will be critical to progress in improving therapeutic and interventional strategies.

Supplementary Material

Refer to Web version on PubMed Central for supplementary material.

Acknowledgements

This work was supported by NIH Grants R01 MH050479 (SFM), R21 MH106817 (MVB), T32 MH016880 (SDD), a NARSAD Young Investigator Grant from the Brain and Behavior Research Foundation (MVB), and a Dissertation

Research Grant from Northeastern University (TMG). The authors thank Alexis Stefano for spine illustrations (Figures 1 and 6) and Nathan Leslie and Isabella Fallon for technical assistance.

References

- Adrian M, Kusters R, Storm C, Hoogenraad CC, and Kapitein LC (2017). Probing the Interplay between Dendritic Spine Morphology and Membrane-Bound Diffusion. *Biophys. J* 113, 2261–2270. [PubMed: 28750887]
- Amat J, Sparks PD, Matus-Amat P, Griggs J, Watkins LR, and Maier SF (2001). The role of the habenular complex in the elevation of dorsal raphe nucleus serotonin and the changes in the behavioral responses produced by uncontrollable stress. *Brain Res.* 917, 118–126. [PubMed: 11602236]
- Amat J, Baratta MV, Paul E, Bland ST, Watkins LR, and Maier SF (2005). Medial prefrontal cortex determines how stressor controllability affects behavior and dorsal raphe nucleus. *Nat. Neurosci* 8, 365–371. [PubMed: 15696163]
- Amat J, Paul E, Zarza C, Watkins LR, and Maier SF (2006a). Previous experience with behavioral control over stress blocks the behavioral and dorsal raphe nucleus activating effects of later uncontrollable stress: role of the ventral medial prefrontal cortex. *J. Neurosci* 26, 13264–13272. [PubMed: 17182776]
- Amat J, Paul E, Zarza C, Watkins LR, and Maier SF (2006b). Previous experience with behavioral control over stress blocks the behavioral and dorsal raphe nucleus activating effects of later uncontrollable stress: role of the ventral medial prefrontal cortex. *J. Neurosci* 26, 13264–13272. [PubMed: 17182776]
- Amat J, Alekseev RM, Paul E, Watkins LR, and Maier SF (2010). Behavioral control over shock blocks behavioral and neurochemical effects of later social defeat. *Neuroscience* 165, 1031–1038. [PubMed: 19909791]
- Bangasser DA, and Wicks B (2017). Sex-specific mechanisms for responding to stress. *J. Neurosci. Res* 95, 75–82. [PubMed: 27870416]
- Baratta MV, Leslie NR, Fallon IP, Dolzani SD, Chun LE, Tamalunas AM, Watkins LR, and Maier SF (2018). Behavioural and neural sequelae of stressor exposure are not modulated by controllability in females. *Eur. J. Neurosci* 47, 959–967. [PubMed: 29359831]
- Baratta MV, Christianson JP, Gomez DM, Zarza CM, Amat J, Masini CV, Watkins LR, and Maier SF (2007). Controllable versus uncontrollable stressors bi-directionally modulate conditioned but not innate fear. *Neuroscience* 146, 1495–1503. [PubMed: 17478046]
- Baratta MV, Zarza CM, Gomez DM, Campeau S, Watkins LR, and Maier SF (2009). Selective activation of dorsal raphe nucleus-projecting neurons in the ventral medial prefrontal cortex by controllable stress. *Eur. J. Neurosci* 30, 1111–1116. [PubMed: 19686468]
- Breslau N, and Kessler RC (2001). The stressor criterion in DSM-IV posttraumatic stress disorder: an empirical investigation. *Biol. Psychiatry* 50, 699–704. [PubMed: 11704077]
- Charney DS (2004). Psychobiological mechanisms of resilience and vulnerability: implications for successful adaptation to extreme stress. *Am. J. Psychiatry* 161, 195–216. [PubMed: 14754765]
- Chen Y, Molet J, Lauterborn JC, Trieu BH, Bolton JL, Patterson KP, Gall CM, Lynch G, and Baram TZ (2016). Converging, Synergistic Actions of Multiple Stress Hormones Mediate Enduring Memory Impairments after Acute Simultaneous Stresses. *J. Neurosci* 36, 11295–11307. [PubMed: 27807170]
- Christianson JP, Paul ED, Irani M, Thompson BM, Kubala KH, Yirmiya R, Watkins LR, and Maier SF (2008). The role of prior stressor controllability and the dorsal raphe nucleus in sucrose preference and social exploration. *Behav. Brain Res* 193, 87–93. [PubMed: 18554730]
- Christianson JP, Thompson BM, Watkins LR, and Maier SF (2009). Medial prefrontal cortical activation modulates the impact of controllable and uncontrollable stressor exposure on a social exploration test of anxiety in the rat. *Stress* 12, 445–450. [PubMed: 19051125]
- Christianson JP, Ragole T, Amat J, Greenwood BN, Strong PV, Paul ED, Fleshner M, Watkins LR, and Maier SF (2010). 5-Hydroxytryptamine 2C Receptors in the Basolateral Amygdala Are Involved in the Expression of Anxiety After Uncontrollable Traumatic Stress. *Biol. Psychiatry* 67, 339–345. [PubMed: 19914601]

- Christianson JP, Flyer-Adams JG, Drugan RC, Amat J, Daut RA, Foilb AR, Watkins LR, and Maier SF (2014). Learned stressor resistance requires extracellular signal-regulated kinase in the prefrontal cortex. *Front. Behav. Neurosci* 8, 348. [PubMed: 25324750]
- Dalla C, Edgecomb C, Whetstone AS, and Shors TJ (2008). Females do not Express Learned Helplessness like Males do. *Neuropsychopharmacology* 33, 1559–1569. [PubMed: 17712351]
- Dolzani SD, Baratta MV, Moss JM, Leslie NL, Tilden SG, Sørensen AT, Watkins LR, Lin Y, and Maier SF (2018). Inhibition of a Descending Prefrontal Circuit Prevents Ketamine-Induced Stress Resilience in Females. *Eneuro* 5, ENEURO.0025–18.2018.
- Farrell MR, Gruene TM, and Shansky RM (2015). The influence of stress and gonadal hormones on neuronal structure and function. *Horm. Behav* 76, 118–124. [PubMed: 25819727]
- Frank AC, Huang S, Zhou M, Gdalyahu A, Kastellakis G, Silva TK, Lu E, Wen X, Poirazi P, Trachtenberg JT, et al. (2018). Hotspots of dendritic spine turnover facilitate clustered spine addition and learning and memory. *Nat. Commun* 9, 422. [PubMed: 29379017]
- Fu M, Yu X, Lu J, and Zuo Y (2012). Repetitive motor learning induces coordinated formation of clustered dendritic spines in vivo. *Nature* 483, 92–95. [PubMed: 22343892]
- Garrett JE, and Wellman CL (2009). Chronic stress effects on dendritic morphology in medial prefrontal cortex: sex differences and estrogen dependence. *Neuroscience* 162, 195–207. [PubMed: 19401219]
- Gruene T, Flick K, Rendall S, Cho JH, Gray J, and Shansky R (2016). Activity-dependent structural plasticity after aversive experiences in amygdala and auditory cortex pyramidal neurons. *Neuroscience* 328.
- Gruene TM, Roberts E, Thomas V, Ronzio A, and Shansky RM (2015). Sex-Specific Neuroanatomical Correlates of Fear Expression in Prefrontal-Amygdala Circuits. *Biol. Psychiatry* 78, 186–193. [PubMed: 25579850]
- Hayashi-Takagi A, Yagishita S, Nakamura M, Shirai F, Wu YI, Loshbaugh AL, Kuhlman B, Hahn KM, and Kasai H (2015). Labelling and optical erasure of synaptic memory traces in the motor cortex. *Nature* 525, 333–338. [PubMed: 26352471]
- Heinsbroek RP, Van Haaren F, Van de Poll NE, and Steenbergen HL (1991). Sex differences in the behavioral consequences of inescapable footshocks depend on time since shock. *Physiol. Behav* 49, 1257–1263. [PubMed: 1896508]
- Jankowski MP, and Sesack SR (2004). Prefrontal cortical projections to the rat dorsal raphe nucleus: Ultrastructural features and associations with serotonin and ?-aminobutyric acid neurons. *J. Comp. Neurol* 468, 518–529. [PubMed: 14689484]
- Kasai H, Matsuzaki M, Noguchi J, Yasumatsu N, and Nakahara H (2003). Structure-stability-function relationships of dendritic spines. *Trends Neurosci.* 26, 360–368. [PubMed: 12850432]
- Kirk RC, and Blampied NM (1985). Activity during inescapable shock and subsequent escape avoidance learning: Female and male rats compared. *NZ. J. Psychol* 14, 9–14.
- Maier SF (2015). Behavioral control blunts reactions to contemporaneous and future adverse events: medial prefrontal cortex plasticity and a corticostriatal network. *Neurobiol. Stress* 1, 12–22. [PubMed: 25506602]
- Maier SF, and Seligman ME (1976). Learned helplessness: Theory and evidence. *J. Exp. Psychol. Gen* 105, 3–46.
- Maier SF, and Watkins LR (2005). Stressor controllability and learned helplessness: the roles of the dorsal raphe nucleus, serotonin, and corticotropin-releasing factor. *Neurosci. Biobehav. Rev* 29, 829–841. [PubMed: 15893820]
- Maier SF, Grahn RE, and Watkins LR (1995). 8-OH-DPAT microinjected in the region of the dorsal raphe nucleus blocks and reverses the enhancement of fear conditioning and interference with escape produced by exposure to inescapable shock. *Behav. Neurosci* 109, 404–412. [PubMed: 7662151]
- Matsuzaki M, Ellis-Davies GC, Nemoto T, Miyashita Y, Iino M, and Kasai H (2001). Dendritic spine geometry is critical for AMPA receptor expression in hippocampal CA1 pyramidal neurons. *Nat. Neurosci* 4, 1086–1092. [PubMed: 11687814]
- Matsuzaki M, Honkura N, Ellis-Davies GCR, and Kasai H (2004). Structural basis of long-term potentiation in single dendritic spines. *Nature* 429, 761–766. [PubMed: 15190253]

- McEwen BS, and Morrison JH (2013). The brain on stress: vulnerability and plasticity of the prefrontal cortex over the life course. *Neuron* 79, 16–29. [PubMed: 23849196]
- McEwen BS, and Stellar E (1993). Stress and the individual. Mechanisms leading to disease. *Arch. Intern. Med* 153, 2093–2101. [PubMed: 8379800]
- Musazzi L, Milanese M, Farisello P, Zappettini S, Tardito D, Barbiero VS, Bonifacino T, Mallei A, Baldelli P, Racagni G, et al. (2010). Acute Stress Increases Depolarization-Evoked Glutamate Release in the Rat Prefrontal/Frontal Cortex: The Dampening Action of Antidepressants. *PLoS One* 5, e8566. [PubMed: 20052403]
- Nava N, Treccani G, Alabsi A, Kaastrup Mueller H, Elfving B, Popoli M, Wegener G, and Nyengaard JR (2015). Temporal Dynamics of Acute Stress-Induced Dendritic Remodeling in Medial Prefrontal Cortex and the Protective Effect of Desipramine. *Cereb. Cortex* 27, bhv254.
- Pereira AC, Lambert HK, Grossman YS, Dumitriu D, Waldman R, Jannetty SK, Calakos K, Janssen WG, McEwen BS, and Morrison JH (2014). Glutamatergic regulation prevents hippocampal-dependent age-related cognitive decline through dendritic spine clustering. *Proc. Natl. Acad. Sci* 111, 18733–18738. [PubMed: 25512503]
- Popoli M, Yan Z, McEwen BS, and Sanacora G (2011). The stressed synapse: the impact of stress and glucocorticoids on glutamate transmission. *Nat. Rev. Neurosci* 13, 22. [PubMed: 22127301]
- Radley JJ, Rocher AB, Rodriguez A, Ehlenberger DB, Dammann M, McEwen BS, Morrison JH, Wearne SL, and Hof PR (2008). Repeated stress alters dendritic spine morphology in the rat medial prefrontal cortex. *J. Comp. Neurol* 507, 1141–1150. [PubMed: 18157834]
- Radley JJ, Anderson RM, Hamilton BA, Alcock JA, and Romig-Martin SA (2013). Chronic stress-induced alterations of dendritic spine subtypes predict functional decrements in an hypothalamo-pituitary-adrenal-inhibitory prefrontal circuit. *J. Neurosci* 33, 14379–14391. [PubMed: 24005291]
- Shansky RM, and Morrison JH (2009). Stress-induced dendritic remodeling in the medial prefrontal cortex: effects of circuit, hormones and rest. *Brain Res* 1293, 108–113. [PubMed: 19361488]
- Shansky RM, Hamo C, Hof PR, McEwen BS, and Morrison JH (2009). Stress-induced dendritic remodeling in the prefrontal cortex is circuit specific. *Cereb. Cortex* 19.
- Shapiro DH, Schwartz CE, and Astin JA (1996). Controlling Ourselves, Controlling Our World. *Am. Psychol* 51, 1213–1230. [PubMed: 8962530]
- Southwick SM, and Charney DS (2012). The science of resilience: Implications for the prevention and treatment of depression. *Science* 338, 79–82. [PubMed: 23042887]
- Steenbergen HL, Heinsbroek RP, Van Hest A, and Van de Poll NE (1990). Sex-dependent effects of inescapable shock administration on shuttlebox-escape performance and elevated plus-maze behavior. *Physiol. Behav* 48, 571–576. [PubMed: 2075210]
- Strong PV, Christianson JP, Loughridge AB, Amat J, Maier SF, Fleshner M, and Greenwood BN (2011). 5-hydroxytryptamine 2C receptors in the dorsal striatum mediate stress-induced interference with negatively reinforced instrumental escape behavior. *Neuroscience* 197, 132–144. [PubMed: 21958863]
- Tanaka J-I, Horiike Y, Matsuzaki M, Miyazaki T, Ellis-Davies GCR, and Kasai H (2008). Protein synthesis and neurotrophin-dependent structural plasticity of single dendritic spines. *Science* 319, 1683–1687. [PubMed: 18309046]
- Varga V, Székely AD, Csillag A, Sharp T, and Hajós M (2001). Evidence for a role of GABA interneurons in the cortical modulation of midbrain 5-hydroxytryptamine neurones. *Neuroscience* 106, 783–792. [PubMed: 11682163]
- Yehuda R, and LeDoux J (2007). Response variation following trauma: a translational neuroscience approach to understanding PTSD. *Neuron* 56, 19–32. [PubMed: 17920012]

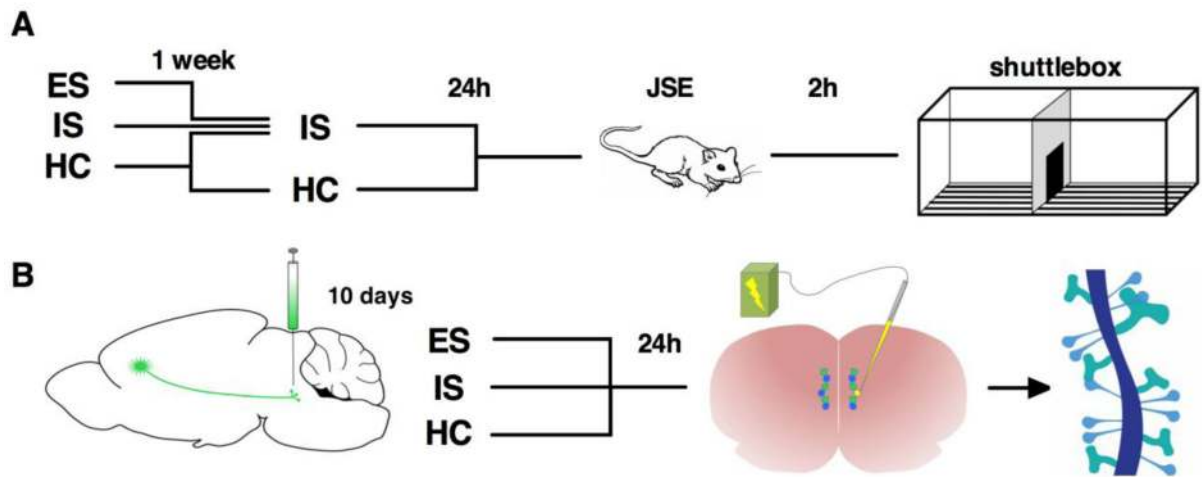


Figure 1. Experimental design.

A) In the behavioral immunization study, animals were exposed to escapable stress (ES), inescapable stress (IS), or home cage (HC) and then left undisturbed for one week. They were then exposed to IS or HC. Twenty-four hours later, animals were tested for juvenile social exploration (JSE), and escape latency and post-shock freezing recovery in an FR-1 shuttlebox. B) For the spine morphology study, animals received stereotaxic injections of fluorescent retrobeads into the DRN, and exposed to ES, IS, or HC 10–14 days later. The next day, animals were euthanized and both retrogradely-labeled layer V prelimbic neurons and unlabeled neighboring neurons were iontophoretically filled with Lucifer Yellow for spine visualization, imaging, and analysis.

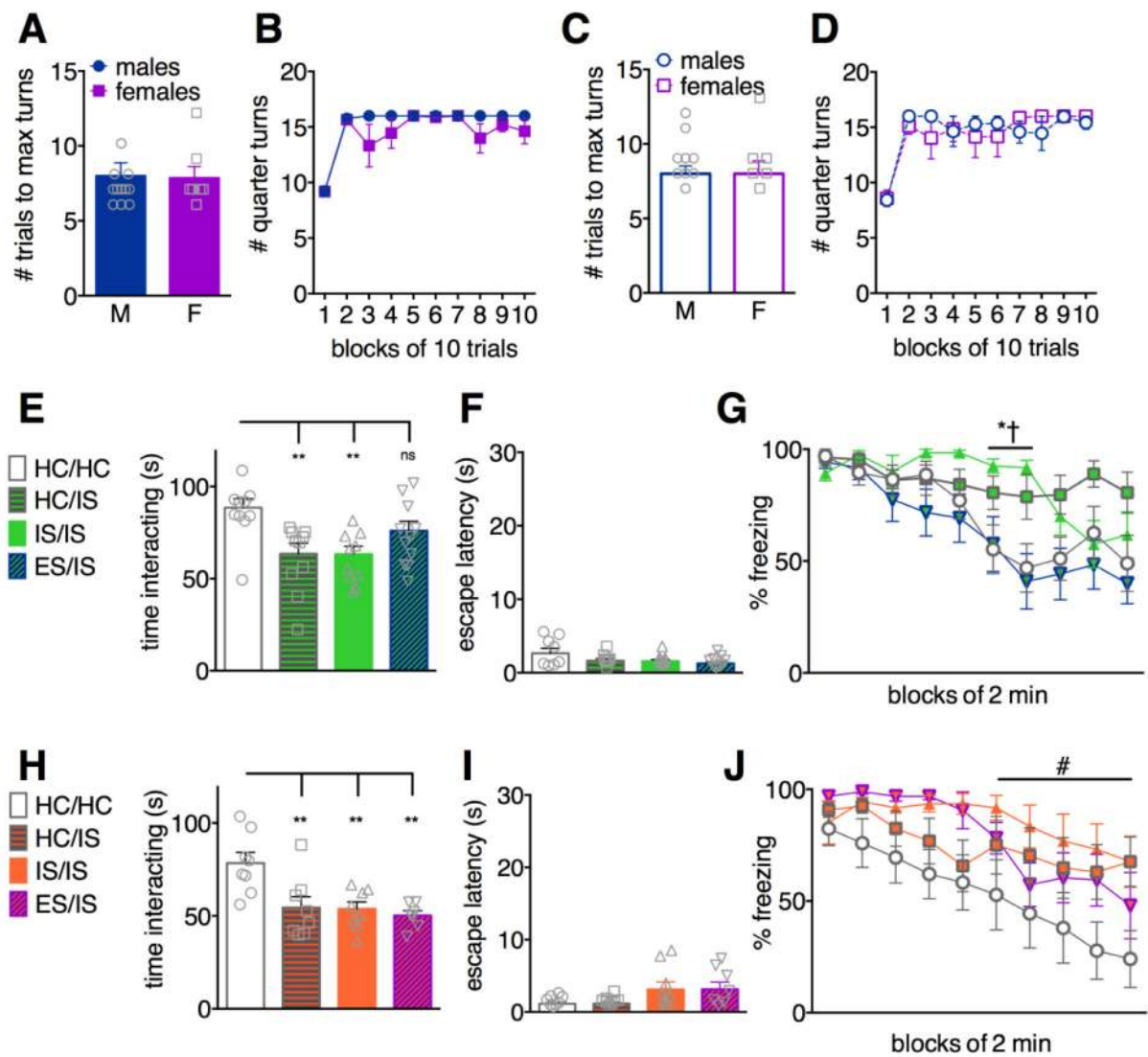


Figure 2. ES immunizes males, but not females, from the behavioral effects of IS.

ES males and females learned to turn the wheel to terminate the shock at the same rate in both the behavioral immunization study (A) and spine morphology study (C), and maintained escape throughout the 100-trial session in both studies (B) and (D). In males, IS reduced time interacting in the JSE test compared to HC/HC controls, an effect partially rescued by prior ES (E). Animals were given a maximum time of 30s to escape footshock (F), but all animals readily escaped and there was no difference across groups in escape latency. IS/IS animals exhibited delayed reduction in freezing compared to ES/IS and HC/HC (G). In females, IS significantly reduced interaction time in the JSE, an effect that was not prevented by ES (H). Escape latency in FR-1 did not differ across stress groups (I). Previous ES exposure did not prevent IS-induced elevated freezing (J). * $p < 0.05$, ** $p < 0.01$ compared to HC. † $p < 0.05$ compared to ES/IS. # $p < 0.05$ IS/IS vs. HC/HC.

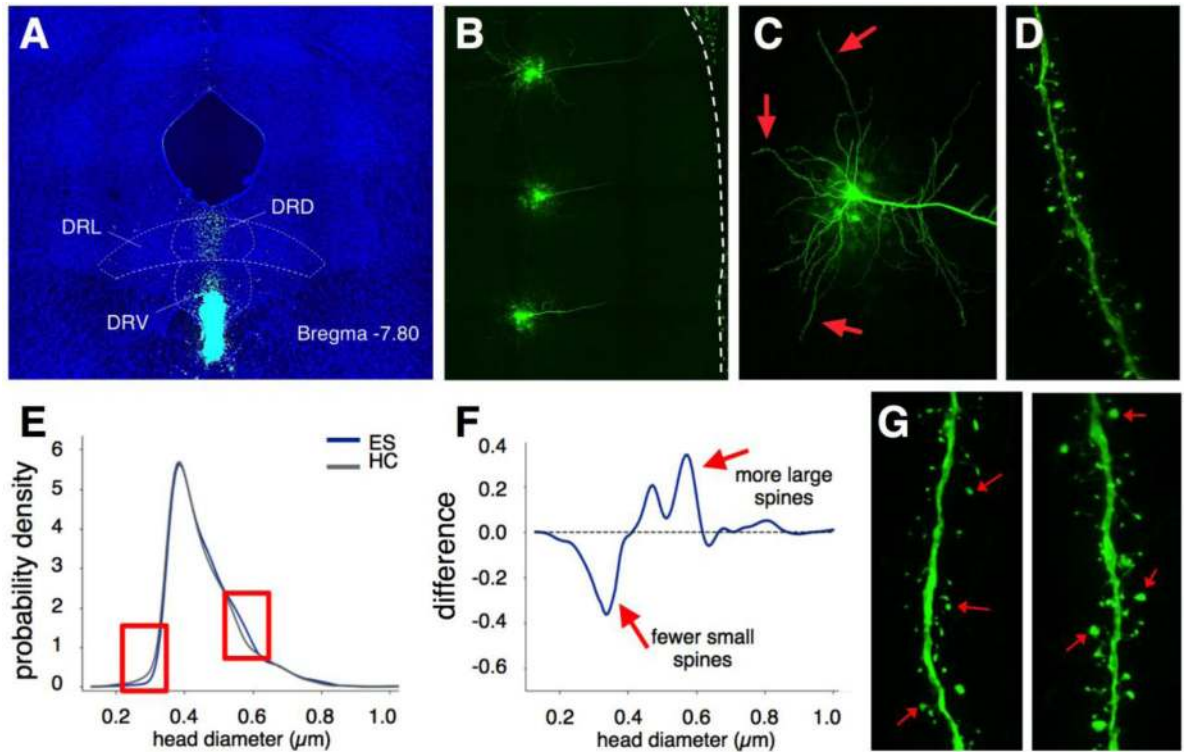


Figure 3. Experimental and analytical approach for identification of circuit-dependent spine plasticity.

A) Representative image of an intra-DRN retrobead injection. B) Representative image of iontophoretically-filled layer V PL neurons. C) Dendritic segments were selected from basal branches (red arrows) and imaged in 3D at 100x (D) for spine head analysis. E) Comparative Kernel density estimates based on cumulative frequency distributions were converted to difference scores (F) to better visualize the specific spine head sizes in which group differences could be observed. This process is illustrated in (E-G) using PL-DRN mushroom spines in HC vs. ES males as an example. Red boxes in (E) identify size-based subpopulations that differ between groups, but as plotted, it is difficult to discern these differences in detail. We therefore plotted the probability density of each experimental group (ES, blue curve) against normalized HC values (dashed line). Where the curved line dips below the dashed line, the experimental group spine population has fewer spines in that size range compared to HC. Where it goes above the dashed line, the experimental group population has more spines in that size range. Compared to PL-DRN dendrites in HC males (G, left) dendrites in ES males (G, right) were populated by more large mushroom spines and fewer small spines. See also Figure 4B.

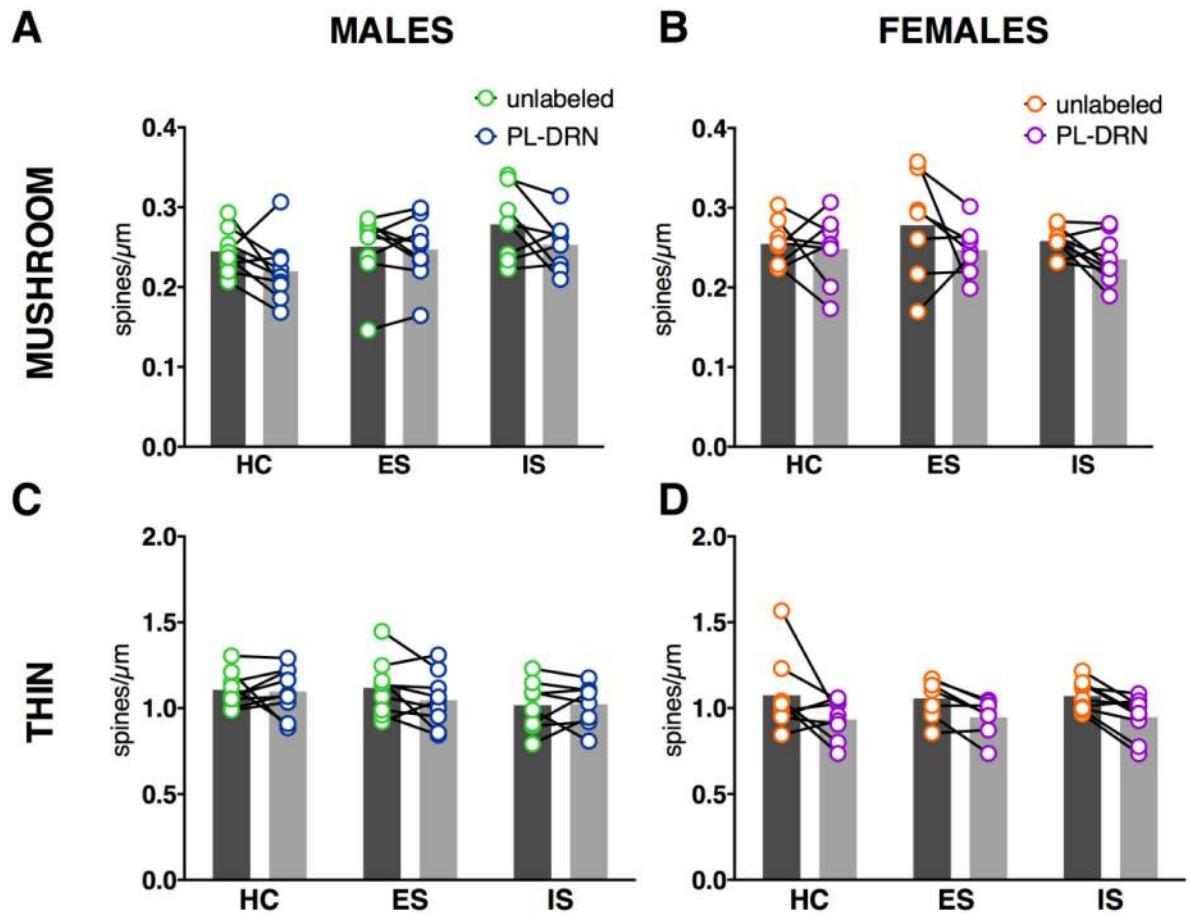


Figure 4. ES and IS do not affect spine densities in either sex.

Means (gray bars) and individual data points for mushroom (A-B) and thin (C-D) spine density in labeled and unlabeled PL neurons for both sexes. Overall, neither IS nor ES affected spine densities in any population. We did observe main effects of circuit in male mushroom spines (A) and in female thin spines (D).

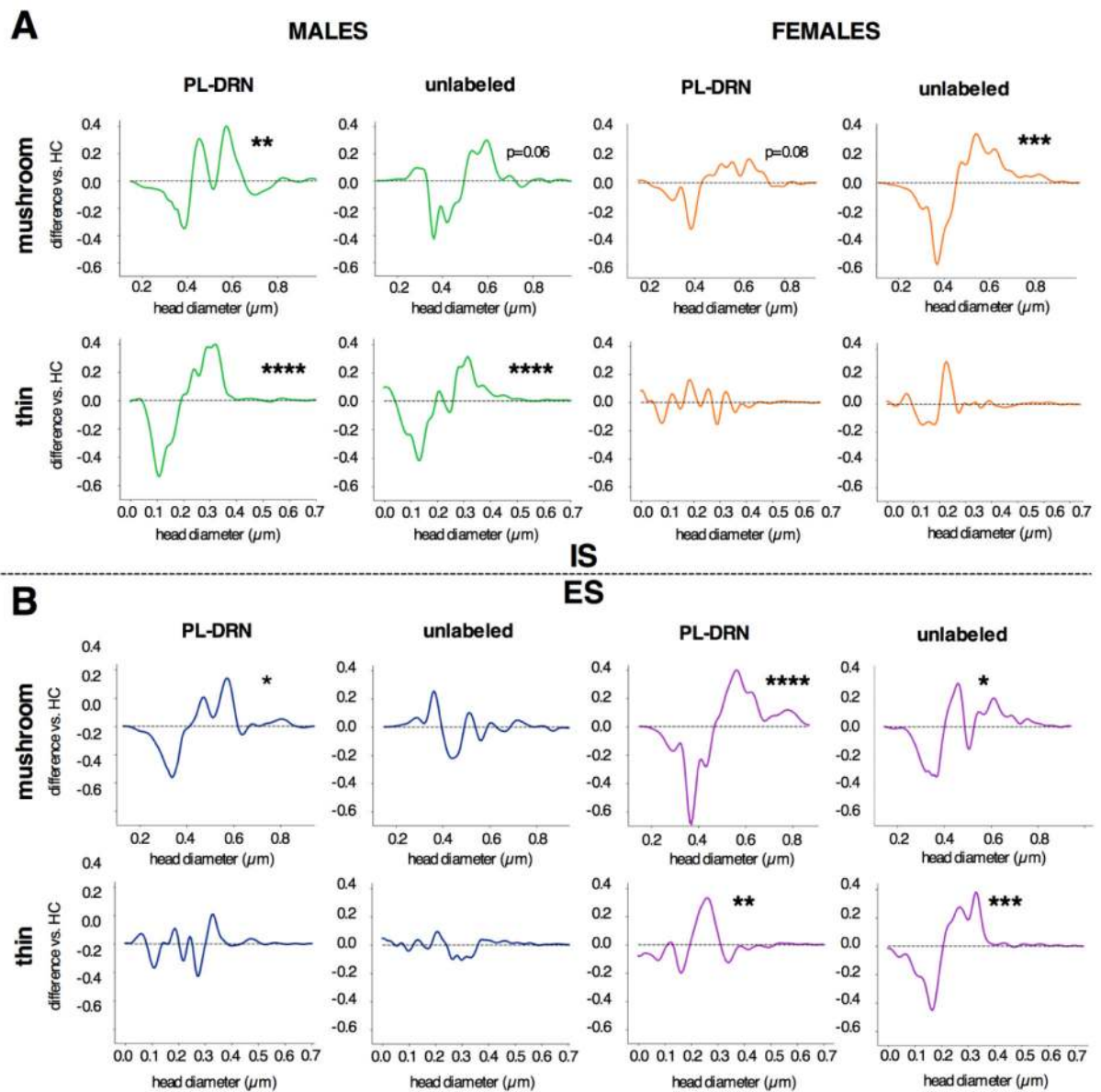


Figure 5. Effects of IS and ES on thin and mushroom spine head diameter in layer V PL neurons.

Plots in (A) represent the effects of IS compared to HC. In males, IS induced non-specific increases in spine head diameter in both mushroom and thin spines. In females, only mushroom spines in unlabeled neurons were affected by IS. In contrast, ES (B) induced a circuit-specific increase in mushroom spine head diameter in males, but a non-specific increase in females, regardless of spine type or circuit. All analyses Kolmogorov-Smirnov tests. * $p < 0.05$; ** $p < 0.01$; *** $p < 0.001$; **** $p < 0.0001$.

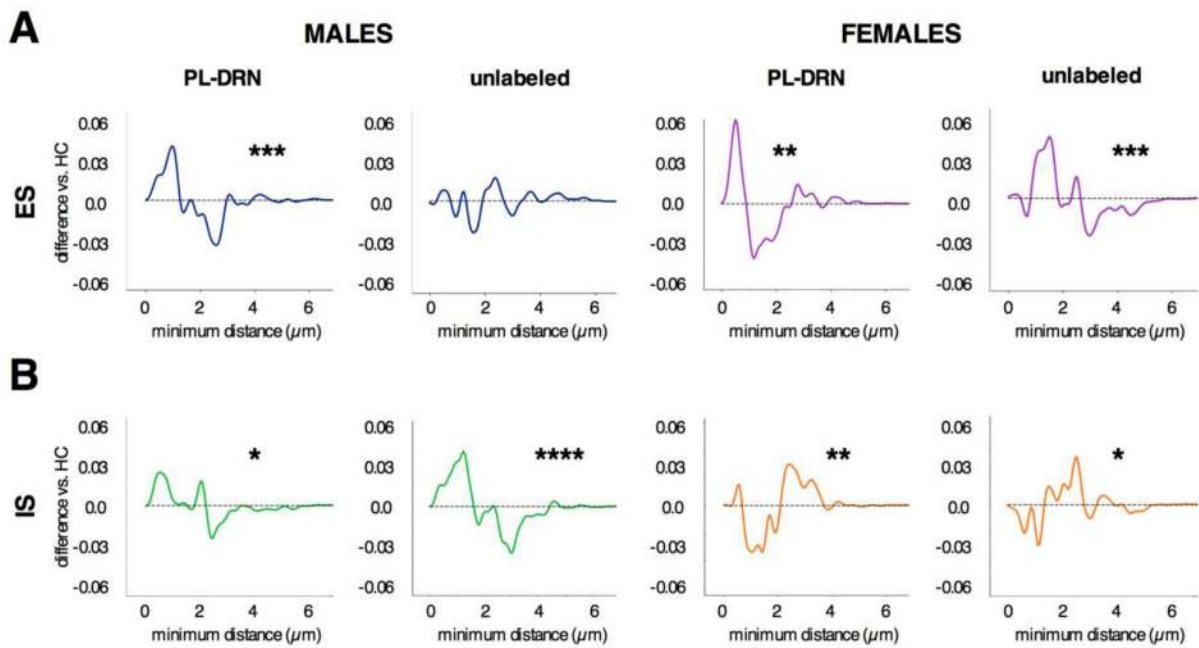


Figure 6. Effects of ES and IS on thin spine clustering in layer V PL neurons.

A) In males, ES induced increased clustering in PL-DRN thin spines only, represented by a greater population of spines with smaller inter-spine distances. In females, ES induced a non-specific increase in clustering. B) IS induced a non-specific increase in clustering in males, but a non-specific decrease in clustering in females. All analyses Kolmogorov-Smirnov tests. * $p < 0.05$; ** $p < 0.01$; *** $p < 0.001$; **** $p < 0.0001$.